

PAPER • OPEN ACCESS

$K^+ \rightarrow \pi^+ \nu \bar{\nu}$: first results from the NA62 experiment at CERN

To cite this article: Cristina Lazzeroni and NA62 Collaboration 2019 *J. Phys.: Conf. Ser.* **1137** 012001

View the [article online](#) for updates and enhancements.



IOP | ebooks™

Bringing you innovative digital publishing with leading voices to create your essential collection of books in STEM research.

Start exploring the [collection](#) - download the first chapter of every title for free.

$K^+ \rightarrow \pi^+ \nu \bar{\nu}$: first results from the NA62 experiment at CERN

Cristina Lazzeroni¹

School of Physics and Astronomy, University of Birmingham, UK

E-mail: cristina.lazzeroni@cern.ch

Abstract. The NA62 experiment at CERN is designed to measure the branching ratio of the $K^+ \rightarrow \pi^+ \nu \bar{\nu}$ decay with unprecedented precision using a decay-in-flight technique, novel for this process. The experiment took data in 2016, 2017 and 2018. Standard model sensitivity is reached using the 2016 data set, allowing a proof-of-principle of the experimental technique.

1. Introduction

The $K^+ \rightarrow \pi^+ \nu \bar{\nu}$ decay are FCNC processes proceeding only through Z penguin and W box diagrams, particularly rare in the Standard Model (SM) due to quadratic GIM mechanism and strong Cabibbo suppression. The decay amplitude is dominated by short-distance dynamics, while the hadronic matrix element can be extracted from the well measured $K^+ \rightarrow e^+ \pi^0 \nu_e$ decays; the rate can therefore be computed with high precision in the SM:

$$BR(K^+ \rightarrow \pi^+ \nu \bar{\nu}) = (8.4 \pm 1.0) \times 10^{-11}$$

¹ On behalf of the NA62 Collaboration: R. Aliberti, F. Ambrosino, R. Ammendola, B. Angelucci, A. Antonelli, G. Anzivino, R. Arcidiacono, M. Barbanera, A. Biagioni, L. Bician, C. Biino, A. Bizzeti, T. Blazek, B. Bloch-Devaux, V. Bonaiuto, M. Boretto, M. Bragadireanu, D. Britton, F. Brizioli, M.B. Brunetti, D. Bryman, F. Bucci, T. Capussela, A. Ceccucci, P. Cenci, V. Cerny, C. Cerri, B. Checcucci, A. Conovaloff, P. Cooper, E. Cortina Gil, M. Corvino, F. Costantini, A. Cotta Ramusino, D. Coward, G. D'Agostini, J. Dainton, P. Dalpiaz, H. Danielsson, N. De Simone, D. Di Filippo, L. Di Lella, N. Doble, B. Dobrich, F. Duval, V. Duk, J. Engelfried, T. Enik, N. Estrada-Tristan, V. Falaleev, R. Fantechi, V. Fascianelli, L. Federici, S. Fedotov, A. Filippi, M. Fiorini, J. Fry, J. Fu, A. Fucci, L. Fulton, E. Gamberini, L. Gatignon, G. Georgiev, S. Ghinescu, A. Gianoli, M. Giorgi, S. Giudici, F. Gonnella, E. Goudzovski, C. Graham, R. Guida, E. Gushchin, F. Hahn, H. Heath, T. Husek, O. Hutanu, D. Hutchcroft, L. Iacobuzio, E. Iacopini, E. Imbergamo, B. Jenninger, K. Kampf, V. Kekelidze, S. Kholodenko, G. Khorauli, A. Khotyantsev, A. Kleimenova, A. Korotkova, M. Koval, V. Kozhuharov, Z. Kucerova, Y. Kudenko, J. Kunze, V. Kurochka, V. Kurshetsov, G. Lanfranchi, G. Lamanna, G. Latino, P. Laycock, C. Lazzeroni, M. Lenti, G. Lehmann Miotto, E. Leonardi, P. Lichard, L. Litov, R. Lollini, D. Lomidze, A. Lonardo, P. Lubrano, M. Lupi, N. Lurkin, D. Madigozhin, I. Mannelli, G. Mannocchi, A. Mapelli, F. Marchetto, R. Marchevski, S. Martellotti, P. Massarotti, K. Massri, E. Maurice, M. Medvedeva, A. Mefodev, E. Menichetti, E. Migliore, E. Minucci, M. Mirra, M. Misheva, N. Molokanova, M. Moulson, S. Movchan, M. Napolitano, I. Neri, F. Newson, A. Norton, M. Noy, T. Numao, V. Obraztsov, A. Ostankov, S. Padolski, R. Page, V. Palladino, C. Parkinson, E. Pedreschi, M. Pepe, M. Perrin-Terrin, L. Peruzzo, P. Petrov, F. Petrucci, R. Piandani, M. Piccini, J. Pinzino, I. Polenkevich, L. Pontisso, Yu. Potrebenikov, D. Protopopescu, M. Raggi, A. Romano, P. Rubin, G. Ruggiero, V. Ryjov, A. Salamon, C. Santoni, G. Saracino, F. Sargeni, V. Semenov, A. Sergi, A. Shaikhiev, S. Shkarovskiy, D. Soldi, V. Sougonyaev, M. Sozzi, T. Spadaro, F. Spinella, A. Sturgess, J. Swallow, S. Trilov, P. Valente, B. Velghe, S. Venditti, P. Vicini, R. Volpe, M. Vormstein, H. Wahl, R. Wanke, B. Wrona, O. Yushchenko, M. Zamkovsky, A. Zinchenko.



where the relevant elements of the Cabibbo-Kobayashi-Maskawa (CKM) matrix are extracted from tree-level processes, and the uncertainty is dominated by the precision on the external inputs [1, 2, 3, 4, 5]. The $K^+ \rightarrow \pi^+ \nu \bar{\nu}$ decay is extremely sensitive to physics beyond the SM, with sizeable deviations expected in various scenarios, like tree-level FCNC mediated by new heavy gauge bosons, models with Lepton Flavour Universality violation, with leptoquarks, or supersymmetric particles [6, 7, 8, 9, 10, 11, 12, 13, 14].

Using a kaon decay-at-rest technique, the experiments E787 [15] and E949 [16] at BNL measured $BR(K^+ \rightarrow \pi^+ \nu \bar{\nu}) = (17.3^{+11.5}_{-10.5}) \times 10^{-11}$.

2. The NA62 experiment

NA62 is a fixed target experiment located at CERN. A schematic view of the apparatus is shown in Figure 1. A primary 400 GeV/c momentum proton beam from the SPS accelerator impinges on a beryllium target, producing a secondary hadron beam selected in momentum (75 ± 0.8 GeV/c) and containing 6% of positive kaons. The momentum of each secondary beam particle is measured by a silicon pixel detector (GTK) and kaons are identified and timestamped by a Cherenkov detector (KTAG). A guard ring detector (CHANTI) vetoes beam inelastic interactions occurring in GTK. A vacuum decay region hosts large-angle photon veto detectors (LAV) and a magnetic spectrometer made by four stations of straw chambers (STRAW) and a dipole magnet. About 10% of positive kaons decays in flight in the 60 m fiducial volume contained in the vacuum decay region. The vacuum region is followed by a RICH detector, to identify timestamp and identify charged decay particles, a scintillator hodoscope (CHOD) used for triggering and timing, and an electromagnetic calorimeter (LKR). Small angle electromagnetic calorimeters (IRC and SAC) improve the photon veto capabilities in the forward region. Hadron calorimeters (MUV1,2) and a plastic scintillator detector (MUV3) are used to suppress muons. A detailed description of the apparatus can be found in [17]. The SPS delivers to the experiment 3.3×10^{12} protons per pulse at full intensity, corresponding to 750 MHz particle rate in GTK. Information from CHOD, RICH, MUV3 and LKR are used to form the online Level0 trigger condition; requirements from KTAG, CHOD, LAV and STRAW are combined to provide the software-based higher level trigger.

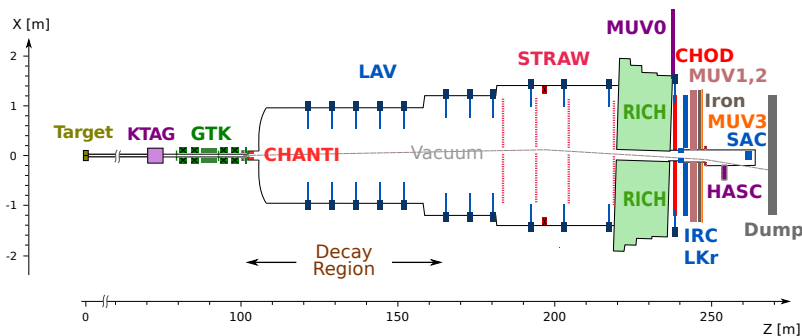


Figure 1. Layout of the NA62 experiment.

3. The $K^+ \rightarrow \pi^+ \nu \bar{\nu}$ analysis

A signal candidate is identified by the presence of a charged kaon in the hadron beam and of a matched (in space and time) charged pion from the kaon decay. The main kinematic variable is the missing mass, m_{miss}^2 , given by the difference squared of the kaon and pion four-momenta (Figure 2). The m_{miss}^2 distributions of the main backgrounds naturally determine two signal

regions. The decay $K^+ \rightarrow \mu^+ \nu$ would have an almost zero m_{miss}^2 corresponding to the neutrino mass, but to be a background the muon must have been wrongly identified as a pion, causing m_{miss}^2 to be negatively distributed. The decay $K^+ \rightarrow \pi^+ \pi^0$, where the two photons from the π^0 decay are lost, has a m_{miss}^2 distribution peaked at the π^0 mass. The decay $K^+ \rightarrow \pi^+ \pi^+ \pi^-$, where two pions are lost, has a m_{miss}^2 at least twice as big as the pion mass. The m_{miss}^2 resolution achieved for the signal is $\sigma(m_{miss}^2) \approx 10^{-3} \text{ GeV}^2/c^4$. Upper and lower limits of the two signal regions (R1 and R2) are chosen about $10 \times \sigma$ away from the m_{miss}^2 distributions of $K^+ \rightarrow \pi^+ \pi^0$, $K^+ \rightarrow \mu^+ \nu$ and $K^+ \rightarrow \pi^+ \pi^+ \pi^-$, in order to minimise background contributions from gaussian tails (Figure 3). The same m_{miss}^2 is also computed taking the charged pion momentum as measured with the RICH instead of the STRAW, or assuming the nominal kaon momentum and direction instead of the GTK measurements. Constraints on these variables are also applied to define signal regions, providing additional power to suppress background coming from tracks mis-reconstructed in STRAW or GTK.

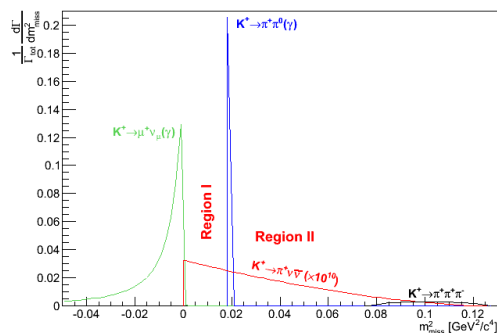


Figure 2. Distributions of m_{miss}^2 for signal and background from the main K^+ decay channels; the backgrounds are normalised according to their branching ratio and the signal is multiplied by a factor 10^{10} .

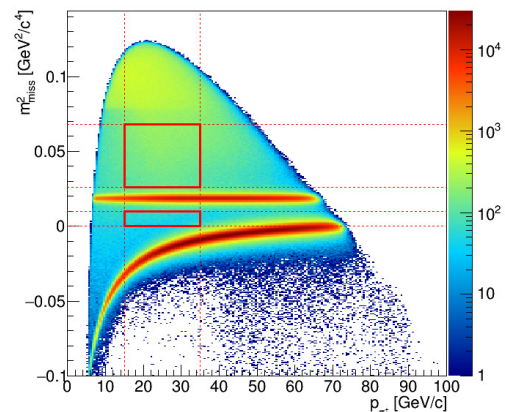


Figure 3. Distribution of m_{miss}^2 as a function of the track momentum, for minimum bias trigger K^+ decay events with single track topology. The contributions from the main K^+ decays are visible. The two kinematic signal regions defined for the analysis (boxes drawn) are indicated for reference.

The signal selection proceeds through K^+ and π^+ identification, and photon and multi-track rejections. The analysis is restricted to $15 < P_{\pi^+} < 35 \text{ GeV}/c$ to improve significantly the π^0 detection and exploit the optimal momentum range for pion identification and muon rejection. The π^+ track is identified combining the information from the RICH detector and the calorimeters (LKr, MUV1-2-3), with an identification efficiency of 64%. Events with in-time extra energy depositions in the LKr are rejected if the corresponding clusters are more than 10 cm away from the impact position of the charged pion on the LKr. Events with hits in the large- or small-angle vetos in time with the π^+ are rejected. Combining downstream information from STRAW, CHODs and LKr, events with extra charged particles in the final state not reconstructed in the spectrometer, or with photons interacting in the material before reaching LKr, LAV and SAV are also rejected. The achieved π^0 detection inefficiency is about 2.5×10^{-8} , measured on data.

The number of kaon decays in the considered 2016 sample is $(1.21 \pm 0.02_{syst}) \times 10^{11}$, measured using a sample of $K^+ \rightarrow \pi^+\pi^0$ decays selected on control data using the same $\pi\nu\bar{\nu}$ criteria, except for the photon and the multiplicity rejection and the cut on m_{miss}^2 . After taking into account the selection acceptance of $(4.0 \pm 0.1)\%$, the trigger efficiency of $(87 \pm 2)\%$ and a random veto loss probability of $(76 \pm 4)\%$, the expected number of identified $K^+ \rightarrow \pi^+\nu\bar{\nu}$ signal events is $(0.267 \pm 0.001_{(stat)} \pm 0.020_{(syst)} \pm 0.032_{(ext)})$, where the external error is due to uncertainties on the SM calculations.

The background is made by all the charged kaon decays and by beam interactions. Background sources are studied with data driven methods in background regions and extrapolated to the signal and control regions, and corrected for kinematic and radiative tails.

The kinematic suppression factor for $K^+ \rightarrow \pi^+\pi^0$ is measured on data with a control sample selected using only the information from LKr to tag the π^0 . The tagging does not bias the resolution tails, but suppresses almost completely the radiative part coming from $K^+ \rightarrow \pi^+\pi^0\gamma$ decays. This radiative contribution is estimated using MC simulation and the measured single photon detection efficiency of the different photon vetoes. Reconstruction tails of $K^+ \rightarrow \mu^+\nu$ are modelled by a control sample selected identifying the μ^+ . Comparison between data and MC suggests that tails are accurately simulated over 5 orders of magnitude. The bias induced by the μ^+ identification and possible correlations between the RICH identification and m_{miss}^2 are taken into account in the systematic uncertainty. Similarly the kinematic tails of $K^+ \rightarrow \pi^+\pi^+\pi^-$ could enter R2 but the combined effect of the multiplicity and kinematic cuts reduces them to an almost negligible level. The background from the rare decay $K^+ \rightarrow \pi^+\pi^-e^+\nu$ (Ke4) is estimated by Monte Carlo, and is suppressed by multiplicity rejection, particle identification and kinematic.

Background can also originate from upstream events in which the charged pion comes from: 1) K^+ decays upstream of the decay region, mostly between GTK stations 2 and 3, matched to a pileup beam particle; 2) interactions of a beam pion mostly with GTK station 3, but also with station 2, matched to a pileup K^+ ; 3) interactions of a K^+ with material in the beam, produced either as prompt particle originating from the interaction or as a decay product of a neutral kaon. This contribution is estimated using a $\pi\nu\bar{\nu}$ -like data sample enriched for upstream events.

The number of expected background events in signal regions (R1 + R2) is reported in Table 1.

Table 1. Summary of the background estimation from the $K^+ \rightarrow \pi^+\nu\bar{\nu}$ analysis of 2016 data.

Process	Expected events in signal region
$K^+ \rightarrow \pi^+\pi^0(\gamma)$	$0.064 \pm 0.007_{stat} \pm 0.006_{syst}$
$K^+ \rightarrow \pi^+\nu(\gamma)$	$0.020 \pm 0.003_{stat} \pm 0.003_{syst}$
$K^+ \rightarrow \pi^+\pi^-e^+\nu$	$0.018^{+0.024}_{-0.017} _{stat} \pm 0.009_{syst}$
$K^+ \rightarrow \pi^+\pi^+\pi^-$	$0.002 \pm 0.001_{stat} \pm 0.002_{syst}$
Upstream background	$0.050^{+0.090}_{-0.030} _{stat}$
Total	$0.15 \pm 0.09_{stat} \pm 0.01_{syst}$

4. Result and Conclusions

The data collected in 2016 amount to about 1% of the total exposure of the NA62 experiment in 2016-2018. One candidate event is found in R2 in the 2016 data sample (Figure 4); this is consistent with the SM expectation (0.267) and with the background expectation (0.15).

The event has a positive track, with momentum of 15.3 GeV/c and ring in the RICH detector consistent with being a pion (Figure 5).

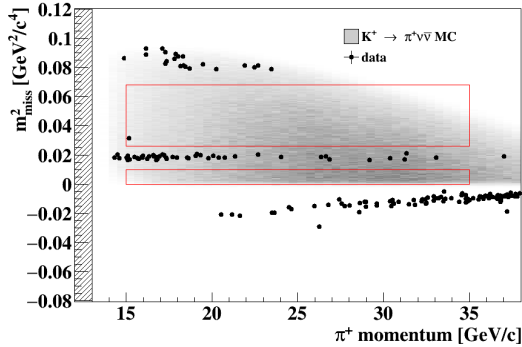


Figure 4. M_{miss}^2 as a function of the π^+ momentum for data passing the $K^+ \rightarrow \pi^+ \nu \bar{\nu}$ selection, except for cuts on m_{miss}^2 and π^+ . The grey area corresponds to the distributions of $K^+ \rightarrow \pi^+ \nu \bar{\nu}$ MC events. The signal regions (red box) are drawn. The unblinding of the signal regions reveals one event observed in R2.

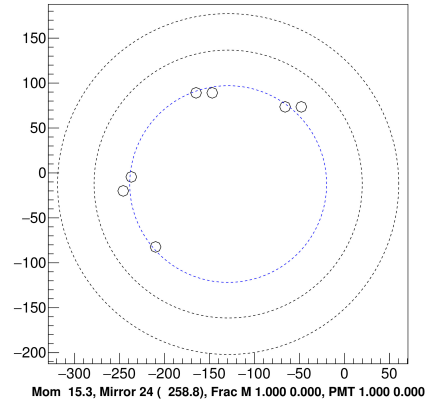


Figure 5. RICH display showing the hits associated to the track for the event observed in R2. The three circles illustrate the positron, muon and pion hypothesis.

With an expected signal of 0.267 events and a background of $(0.15 \pm 0.09_{stat} \pm 0.01_{syst})$ events, a hybrid frequentistic-bayesian prescription [18] is applied to account for the uncertainty on the expected background. Using the CL_s method [19], the observed upper limit on the $K^+ \rightarrow \pi^+ \nu \bar{\nu}$ branching ratio is $BR(K^+ \rightarrow \pi^+ \nu \bar{\nu}) < 14 \times 10^{-10}$ at 95% CL, while the corresponding expected limit is $BR(K^+ \rightarrow \pi^+ \nu \bar{\nu}) < 10 \times 10^{-10}$.

The result presented here represents a proof of principle of the novel decay-in-flight technique adopted by NA62. The NA62 experiment has already collected more than 20 times the statistics presented here, and the analysis of this larger data sample is in progress.

References

- [1] Buras A, Buttazzo D, Girrbach-Noe J and Knegjens R 2015 *JHEP* **1511** 33.
- [2] Buchalla G and Buras A 1999 *Nucl. Phys. B* **548** 309.
- [3] Buras A, Gorbhan M, Haisch U and Nierste U 2006 *JHEP* **11** 002.
- [4] Brod J, Gorbahn M and Stamou E 2011 *Phys. Review D* **83** 034030.
- [5] Isidori G, Mescia F and Smith C 2005 *Nucl. Phys. B* **718** 319.
- [6] Mescia F and Smith C 2007 *Phys. Review D* **76** 034017.
- [7] Blanke M, Buras A and Recksiegel S 2016 *Eur. Phys. J. C* **76** no.4 182.
- [8] Blanke M, Buras A, Duling B, Gemmler K and Gori S 2009 *JHEP* **0903** 108.
- [9] Buras A, Buttazzo D and Knegjens R 2015 *JHEP* **1511** 166.
- [10] Isidori G, Mescia F, Paradisi P, Smith C and Trine S 2006 *JHEP* **0608** 064.
- [11] Blazek T and Matak P 2010 *Nucl. Phys. Proc. Suppl.* **198** 216.
- [12] Tanimoto M and Yamamoto K 2016 *PTEP* no.12 123B02.
- [13] Bordone M, Buttazzo D, Isidori G and Monnard J 2017 *Eur. Phys. J. C* **77** no.9 618.
- [14] Bobeth C and Buras A 2018 *JHEP* **1802** 101.
- [15] Artamonov A et al 2008 *Phys. Rev. Lett.* **101** 191802.
- [16] Artamonov A et al 2008 *Phys. Rev. D* **79** 092004.
- [17] Cortina-Gil E et al 2017 *J. Instrum.* **12** P05025.
- [18] Cousins R et al. 2008 *Nucl. Instrum. Methods A* **529** 480.
- [19] Read A 2002 *J. Phys. G* **28** 2693.